

# PROCEEDINGS OF SPIE

[SPIDigitalLibrary.org/conference-proceedings-of-spie](https://spiedigitallibrary.org/conference-proceedings-of-spie)

## Graphene-based photodetector at room temperature

V. X. Ho, Y. Wang, M. P. Cooney, Vinh Q. N.

V. X. Ho, Y. Wang, M. P. Cooney, Vinh Q. N., "Graphene-based photodetector at room temperature," Proc. SPIE 10729, Optical Sensing, Imaging, and Photon Counting: From X-Rays to THz, 1072907 (20 September 2018); doi: 10.1117/12.2320922

**SPIE.**

Event: SPIE Nanoscience + Engineering, 2018, San Diego, California, United States

# Graphene-Based Photodetector at Room Temperature

V. X. Ho<sup>1</sup>, Y. Wang<sup>1</sup>, M. P. Cooney<sup>2</sup>, and N. Q. Vinh<sup>1\*</sup>

<sup>1</sup> Department of Physics and Center for Soft Matter and Biological Physics, Virginia Tech, Blacksburg, VA 24061, USA

<sup>2</sup> NASA Langley Research Center, Hampton, Virginia 23681, USA

\* Corresponding author: [vinh@vt.edu](mailto:vinh@vt.edu); phone: 1-540-231-3158

## ABSTRACT

There are a growing number of applications demanding high sensitivity visible to mid-infrared photodetectors operating at room temperature. Graphene is ideally suitable for optoelectronic photodetectors sensitive from visible to mid-infrared frequencies. Here we report the integration of graphene with thin film high- $\kappa$  dielectric layers prepared by e-beam thermal evaporation, sputtering deposition and atomic layer deposition methods for the graphene field-effect transistor photodetector development. The impact of dielectric layers on graphene properties and the operation of photodetectors varies based on the choice of dielectric and deposition parameters. This work provides a route for use of graphene in the infrared detection at room temperature.

**Keywords:** Graphene, Atomic Layer Deposition, Photodetectors

## 1. INTRODUCTION

The ability to convert light into electronic signals exists in a narrow range of frequencies from ultraviolet, visible and infrared (near and far) regions. For example, Cs-I, AlGaIn, Si, Ge, InGaAs are used for photodetectors in the ultraviolet, visible and near-infrared regions, while the mid- and far-infrared photodetectors typically depend on small-bandgap semiconductors including PbS, PbSe or HgCdTe, and thermal photo-detection techniques. In contrast to these materials, graphene with its gapless bandgap structure is a great candidate material for broad band photodetectors.[1-4] The unique carrier multiplication, a process that generates multiple charge carriers from the absorption of a single photon, and extremely short carrier lifetime allow for high-speed photodetectors in a wide spectral range from ultraviolet to the far infrared region.[2, 5] Therefore, to generate a photocurrent and reduce the heating of graphene layers, efficient separate of carriers (electrons and holes) at the pico-second timescale is required.

A large number of successful graphene photodetectors have been demonstrated.[1, 4, 6] However, the small photo-absorption volume of the monolayer graphene, the sub-picosecond lifetime, and uniform high- $\kappa$  dielectric layers on graphene have proven challenging in practical applications.[7-9] With a drain bias applied to graphene field-effect transistor (FET) photodetectors, a typical dark-current reaches the order of micro to milliamps. The graphene dark-current value is several orders of magnitudes larger than the typical dark-current of Si photodetectors, on an order of nano-amps. To manufacture practical graphene FET photodetectors, a high quality of the dielectric layer on top of graphene is required for electrostatic gates. This layer should be ultra-thin of a few nanometers thick and very uniform without any pinholes. At the same time, the dielectric layer should possess high dielectric constant,  $\kappa$ , high breakdown voltage and low leakage current. The high- $\kappa$  dielectric layers in graphene FET photodetectors also enhance charge carrier mobility due to the reduced Coulombic scattering of charge carriers.[10, 11]

Thermal atomic layer deposition (ALD) provides ultra-thin, uniform, and high-quality films with sub-monolayer thickness control of high- $\kappa$  dielectric layers on graphene.[7, 12] The gate dielectric layers at temperatures below 250°C using the ALD technique has shown to be an excellent method toward the integration of dielectric layers with graphene. In this work, we report graphene photodetectors fabricated with a high- $\kappa$  dielectric layer ( $\text{Al}_2\text{O}_3$ ) on graphene using three methods including e-beam thermal evaporation, sputtering and atomic layer deposition. The photocurrent response from devices with an ALD  $\text{Al}_2\text{O}_3$  dielectric layer on graphene is reported.

## 2. METHODS AND EXPERIMENTAL DETAILS

### 2.1. Device fabrication

The monolayer graphene on copper foils from Grolltex in this work was transferred onto a Si/SiO<sub>2</sub> substrate.[13] We used the *p*-doped (1 – 10  $\Omega\cdot\text{cm}$ ) Si wafer under a 285-nm-thick SiO<sub>2</sub> layer as the back gate. We transferred the chemical vapor deposition (CVD) graphene film on top of the wafer using a poly-(methyl-methacrylate) (PMMA) wet transfer method. The single-layer of graphene film was confirmed by the Raman spectroscopy. Using photolithography and oxygen plasma etching processes, we fabricated the graphene layer on the silicon wafer. The graphene film was patterned into (55 × 50)  $\mu\text{m}^2$ . Metal source and drain contacts (Cr/Au with 10/50 nm thickness) for transport measurements were deposited directly onto the wafer by optical lithography to form FETs with a (50 × 50)  $\mu\text{m}^2$  channel area. We have used several techniques to deposit an 80-nm dielectric layer ( $\text{Al}_2\text{O}_3$ ) on graphene including e-beam thermal evaporation, sputtering deposition and ALD. Finally, a narrow strip of 50-nm-thick Cr/Au film for the top gate was created in the same method as the graphene contacts.

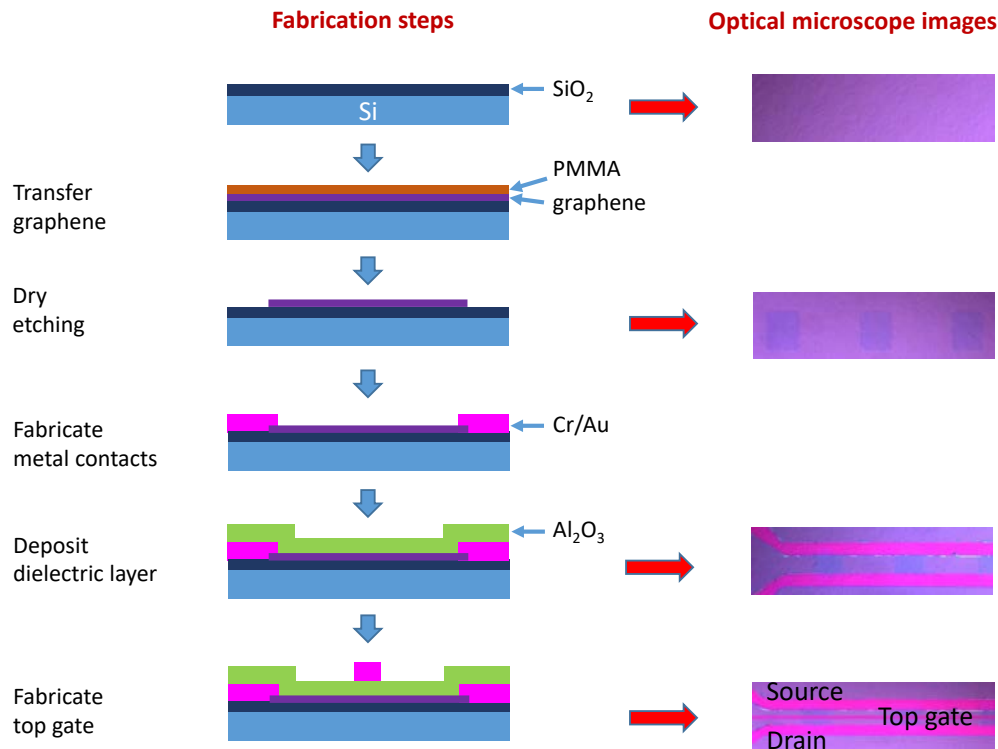


**Figure 1:** Fabrication processes together with optical microscope images of each step to fabricate graphene FET photodetectors: growing a dielectric SiO<sub>2</sub> layer on a Si wafer; transferring graphene with a PMMA layer; oxygen plasma etching with photoresist masks defined by photolithography; fabricating Cr/Au source and drain contacts; deposition of Al<sub>2</sub>O<sub>3</sub> dielectric layer on graphene; formation of graphene FET photodetectors with a narrow Cr/Au top gate.

Figure 1 shows fabrication steps and optical microscope images of graphene photodetector devices. In the dielectric deposition approach below, the high- $\kappa$   $\text{Al}_2\text{O}_3$  dielectric area was created larger than the electrical contact area including graphene, source and drain contacts and the top gate electrode. The top gate is well separated and no electrical connection exists between the top gate electrode and the graphene area including source and drain contacts. Since the thickness of the dielectric layer is similar with metal contacts, the dielectric layer may not completely cover the electrical contacts, and a discontinuity of the oxide layer can occur at the contact edges. When the gate metal is deposited on the damaged area, a low-resistance or short-circuit between the top gate electrode and the electrical contacts will occur. To prevent this, we ensure a gap between the electrical contact area and the top gate.

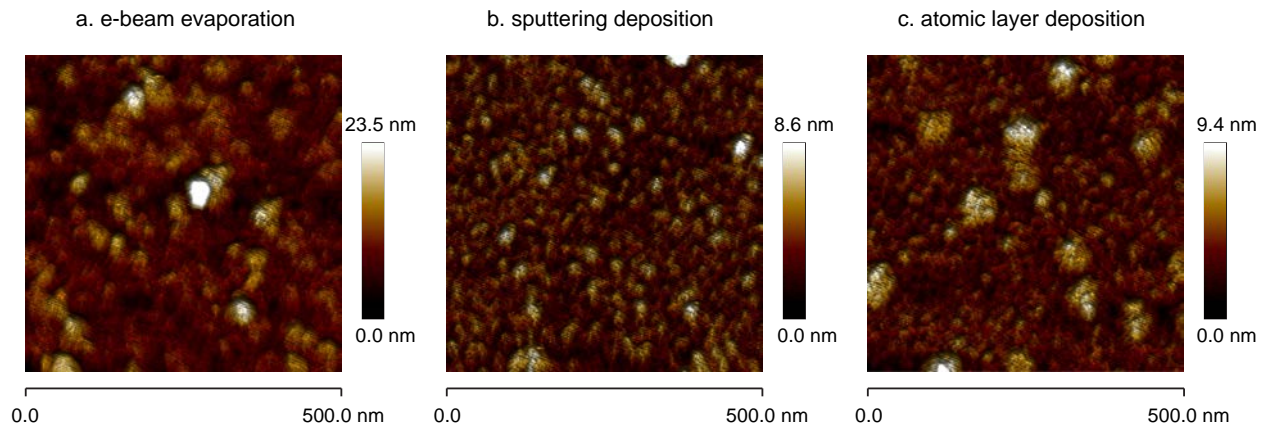


**Figure 2:** Atomic force microscopy images of  $\text{Al}_2\text{O}_3$  films deposited on CVD graphene using (a) an electron beam, thermal evaporation, (b) sputtering deposition, and (c) thermal atomic layer deposition.

## 2.2. Methods to obtain high- $\kappa$ dielectric layers

The operation of the device depends strongly on the dielectric layer on graphene.[12] We have employed several methods including e-beam thermal evaporation, sputtering deposition and atomic layer deposition to deposit a dielectric layer on graphene. Specifically, we have used an aluminum oxide ( $\text{Al}_2\text{O}_3$ ,  $\epsilon_r = 9$ ) dielectric layer on graphene. The high- $\kappa$  dielectric layer in graphene-based photodetector reduces Coulombic charge carrier scattering [10] and enhance the mobility of charge carriers [11]. We present techniques to deposit the high- $\kappa$  dielectric layer ( $\text{Al}_2\text{O}_3$ ) on CVD graphene and compare their surfaces.

*E-beam thermal evaporation* method is a simple and economical approach to obtain a dielectric layer. However the quality as well as the uniform of the layer will be an issue for the gate dielectric in field-effect transistors. Typically, an  $\text{AlO}_x$  dielectric will form in the device after the thermal evaporation process and an  $\text{Al}_2\text{O}_3$  dielectric layer will be created with post-passivation steps.[14] We have used the PVD 250 thin film deposition system (Kurt J. Lesker) to produce an  $\text{Al}_2\text{O}_3$  dielectric layer. Figure 2a shows a typical AFM image of the surface of  $\text{Al}_2\text{O}_3$  dielectric layer on graphene. The image shows a rough surface when we compared with those from the sputtering deposition and ALD techniques.

*Sputtering deposition* technique has been used to produce high-quality dielectric layers. This method is economically more favorable than the ALD technique.[15, 16] For this method, we have employed the PVD 75 (Kurt J. Lesker) operating in the magnetron sputtering option. Figure 2b shows a typical AFM image of the surface of  $\text{Al}_2\text{O}_3$  dielectric layer on graphene. The image shows a better surface when we compared with those from the e-beam thermal evaporation.

*Thermal atomic layer deposition* provides high-quality dielectric layers with a precisely defined thickness. At temperatures below 250 °C, the ALD method has been demonstrated as an excellent method for the integration of dielectric layers with graphene.[7] Because this technique is a water-based method, the graphene surface must undergo preparation that results in non-uniform dielectric deposition. To overcome this issue, several additional steps are

added, in which the surface of graphene is pretreated before the deposition of a dielectric layer.[17] The pretreated deposition method has resulted in uniform  $\text{Al}_2\text{O}_3$  dielectric coverage.[14, 17] In this work, we have employed the same approach for ALD technique. A typical AFM image of the surface of  $\text{Al}_2\text{O}_3$  dielectric layer on graphene is shown in Figure 2c. The quality of the dielectric layer using this technique is similar to the sputtering deposition method.

### 3. RESULTS AND DISCUSSIONS

We focus in this report on our analysis of the graphene FET photodetectors with the  $\text{Al}_2\text{O}_3$  dielectric layer fabricated using the ALD method. To evaluate the influence of the dielectric layer on quality of graphene, we used Raman spectroscopy. A Raman spectrum was obtained by using a WITec UHTS 300 micro-Raman spectrometer equipped with a CCD detector and a  $100\times$  objective lens (NA 0.90). The graphene sample was excited by a laser operating at 663.1-nm wavelength. Figure 3 shows the Raman spectrum of a CVD monolayer graphene on  $\text{Si}/\text{SiO}_2$  covered by an ALD  $\text{Al}_2\text{O}_3$  dielectric layer. The Raman spectrum shows two main peaks at  $\sim 1592\text{ cm}^{-1}$  (G) and  $\sim 2669\text{ cm}^{-1}$  (2D). A lower peak (D) can be observed at  $1345\text{ cm}^{-1}$ , which indicates graphene defects. The 2D to G intensity ratio,  $I_{2D}/I_G$ , is 5.3. The high value confirms a high quality of graphene layer on the photodetector. Comparing with the graphene in copper, the intensity of the G line reduces significantly and the position of this peak shifts towards a higher wavenumber, indicating a single layer graphene in our device.[18] The intensity ratio of D to G,  $I_D/I_G$ , is correlated to the deposition process and the oxidation of the ALD dielectric layer. This ratio value of 0.3 indicates a normal density of lattice defects in the  $\text{Al}_2\text{O}_3$  dielectric layer covered graphene.[15]

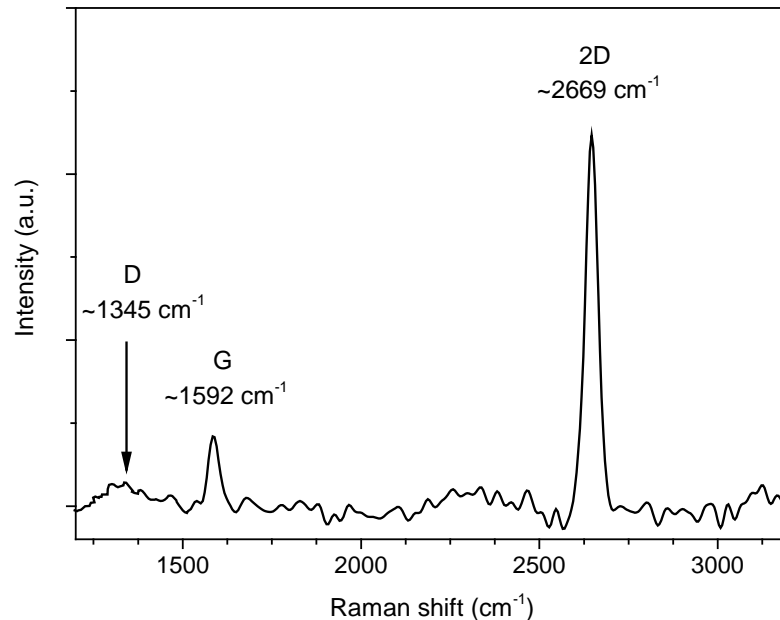


**Figure 3:** Raman spectrum of a graphene device on  $\text{SiO}_2$  substrate with an ALD  $\text{Al}_2\text{O}_3$  dielectric layer on the top surface.

The electrical characteristics of the graphene FET photodetectors were characterized by a semiconductor characterization system (Keithley 4200A-SCS) and the optical properties of the photodetectors were investigated under illumination of a Tungsten-Halogen lamp. The intensity of the light source was measured with a thermopile sensor (Newport 919P).

Figure 4 shows optical microscope image and corresponding electrical and optical measurement results for our graphene FET photodetector. At gate voltages of 0 V, the drain current,  $I_d$ , was measured as a function of the drain voltage,  $V_d$ , for different ranges of  $V_d$  sweeping as shown in Figure 4b. All the curves were obtained after the metal

contact lift-off process without any post-fabrication treatment including current or thermal annealing. These curves well overlap for various sweeping ranges, indicating that electrical contacts between the source/drain and graphene are very stable. The field effect measurement results of the graphene FEL photodetector have been characterized (Figure 4c). The transfer curve (the drain current,  $I_d$ , as a function of the back gate voltage,  $V_{bg}$ ) under the dark condition is reproducible, and the minimum of the conductivity related to the Dirac point is close to 0 V. The result suggests that a contamination on graphene surface during the transfer process of graphene is very low. Thus, the performance of the device is repeatable without any post-treatment processes.

To examine the performance of FETs fabricated from graphene films covered with  $\text{Al}_2\text{O}_3$  dielectrics using ALD method, four devices have been measured and the distribution of the Dirac point of these devices was plotted in Figure 4c, inset. The Dirac points of these devices are ranging from -4 to -8 V. This result indicates that the uniformity of our devices was improved by the ALD  $\text{Al}_2\text{O}_3$  dielectric layer.

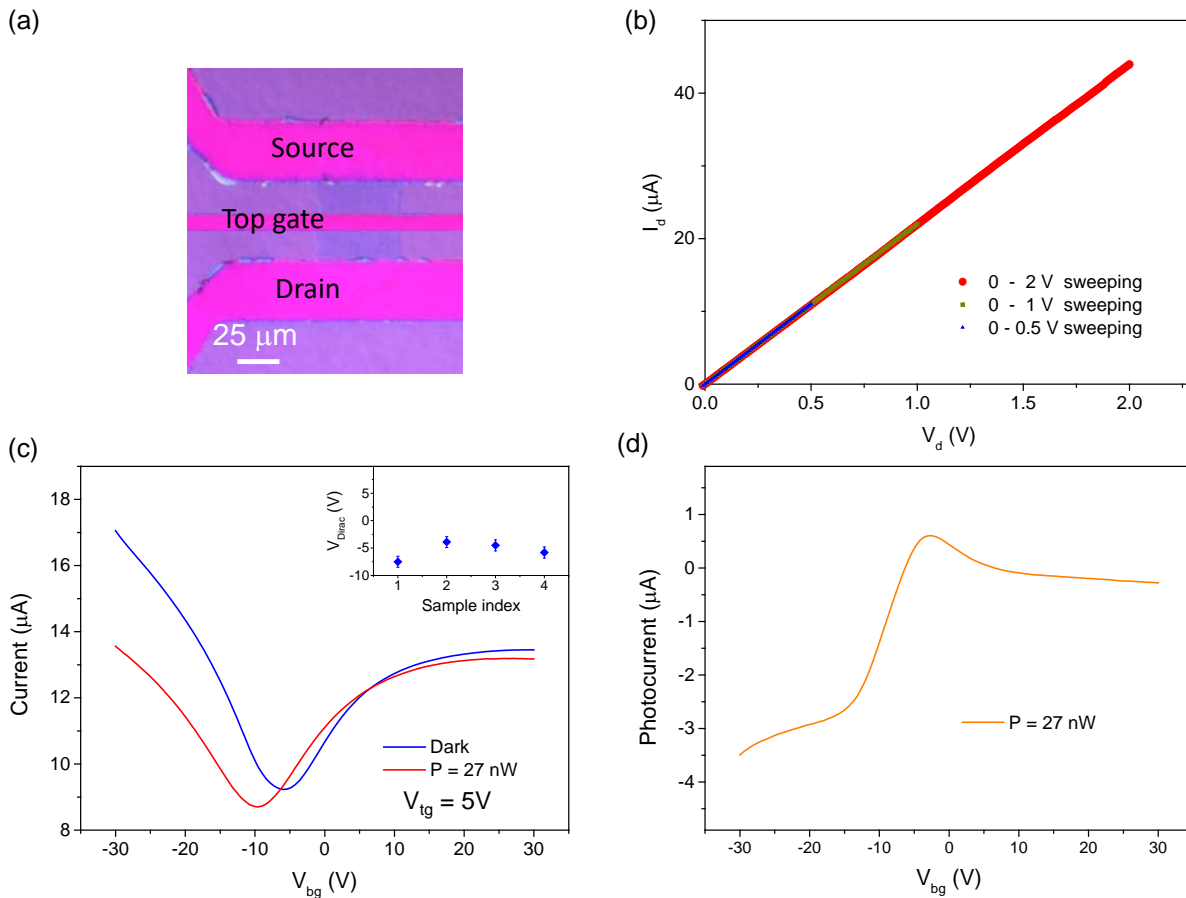


**Figure 4:** Electrical and optical properties of graphene FET photodetectors using an ALD  $\text{Al}_2\text{O}_3$  dielectric layer. (a) Optical microscope image of a typical graphene FET photodetector. (b)  $I_d$ - $V_d$  curves obtained at gate voltages of 0 V for various ranges of  $V_d$  sweeping. (c)  $I_d$ - $V_{bg}$  characteristics of the graphene FET photodetector under different conditions (dark and a broad band light source with a power of 27 nW). The potential of the top gate was at 5 V, and the source-drain bias voltage  $V_{sd} = 0.5$  V. The broad band light source (Tungsten-Halogen lamp) with the peak emission at 850 nm and a spot size of 15 mm covered the whole graphene FET photodetector. Distribution of Dirac point of photodetector devices from graphene covered with an ALD dielectric  $\text{Al}_2\text{O}_3$  layer is shown in the inset. (d) Photocurrent as a function of back gate voltage using the broad band light source with a power of 27 nW.

To estimate the response of graphene photo-detection using an ALD Al<sub>2</sub>O<sub>3</sub> dielectric layer, we have determined the photocurrent of the graphene FET photodetectors.

The effect of light illumination on the graphene devices is shown in the Figure 4c. Specifically, we observed the photocurrent,  $I_{sd}$ , as a function of the back gate voltage,  $V_{bg}$ . We used a broad band light source (Tungsten-Halogen lamp) with the peak emission at 850 nm. The spot size of the beam is large. We have used a diaphragm with a diameter of 15 mm to form a light source with a uniform intensity distribution. The light source covers the whole graphene FET photodetector with a size of 50 x 50  $\mu\text{m}^2$ . The power of the light source is 0.95 mW. Thus, the power of the light source on the active area of the graphene photodetector in the experiment was estimated of 27 nW. The potential of the top gate,  $V_{tg}$ , was at 5 V, and the source-drain bias voltage,  $V_{sd}$ , was set at 0.5 V. As can be seen from Figure 4c, the transfer characteristic curve shifts toward negative voltage of the back gate,  $V_{bg}$ , with illumination of light, and a shift of the Dirac point voltage of 5 V is observed.

The net photocurrent can be obtained by subtracting the dark-current from the illumination current ( $I_{\text{illumination}} - I_{\text{dark}}$ ), and is plotted in Fig. 4d. A net photocurrent of  $\sim 3 \mu\text{A}$  has been observed at  $V_{bg} = -20 \text{ V}$  and  $V_{sd} = 0.5 \text{ V}$ . Thus, the photoresponsivity of our graphene detector of 130 A/W has been measured. This value is the same order of magnitude when compared with other report of graphene photodetector in the infrared region.[4]

## 4. CONCLUSIONS

Here we have reported the deposition a thin film high- $\kappa$  Al<sub>2</sub>O<sub>3</sub> dielectric layer on graphene for field-effect transistor photodetector development. The device can detect a low power from a broad band light source in the infrared region with the photoresponsivity of 130 A/W. Our work provides a route for the utilization of graphene for infrared sensing at room temperature.

## ACKNOWLEDGMENT

The authors gratefully acknowledge the financial support of this effort by the IRAD program from NASA Langley Research Center's Office of Chief Technologist.

## REFERENCES

- [1] Zhang, Y. B., Tang, T. T., Girit, C., Hao, Z., Martin, M. C., Zettl, A., Crommie, M. F., Shen, Y. R., and Wang, F., "Direct observation of a widely tunable bandgap in bilayer graphene," *Nature*, 459, 820-823, (2009).
- [2] Xia, F. N., Mueller, T., Lin, Y. M., Valdes-Garcia, A., and Avouris, P., "Ultrafast graphene photodetector," *Nature Nanotechnology*, 4, 839-843, (2009).
- [3] Bonaccorso, F., Sun, Z., Hasan, T., and Ferrari, A. C., "Graphene photonics and optoelectronics," *Nature Photonics*, 4, 611-622, (2010).
- [4] Liu, C. H., Chang, Y. C., Norris, T. B., and Zhong, Z. H., "Graphene photodetectors with ultra-broadband and high responsivity at room temperature," *Nature Nanotechnology*, 9, 273-278, (2014).
- [5] Dawlaty, J. M., Shivaraman, S., Chandrashekhara, M., Rana, F., and Spencer, M. G., "Measurement of ultrafast carrier dynamics in epitaxial graphene," *Applied Physics Letters*, 92, 042116, (2008).
- [6] Farmer, D. B., Chiu, H. Y., Lin, Y. M., Jenkins, K. A., Xia, F. N., and Avouris, P., "Utilization of a Buffered Dielectric to Achieve High Field-Effect Carrier Mobility in Graphene Transistors," *Nano Letters*, 9, 4474-4478, (2009).
- [7] Vervuurt, R. H. J., Kessels, W. M. M., and Bol, A. A., "Atomic Layer Deposition for Graphene Device Integration," *Advanced Materials Interfaces*, 4, 1700232, (2017).
- [8] Nair, R. R., Blake, P., Grigorenko, A. N., Novoselov, K. S., Booth, T. J., Stauber, T., Peres, N. M. R., and Geim, A. K., "Fine structure constant defines visual transparency of graphene," *Science*, 320, 1308-1308, (2008).
- [9] Urich, A., Unterrainer, K., and Mueller, T., "Intrinsic Response Time of Graphene Photodetectors," *Nano Letters*, 11, 2804-2808, (2011).

- [10] Jang, C., Adam, S., Chen, J. H., Williams, D., Das Sarma, S., and Fuhrer, M. S., "Tuning the effective fine structure constant in graphene: Opposing effects of dielectric screening on short- and long-range potential scattering," *Physical Review Letters*, 101, 146805, (2008).
- [11] Chen, F., Xia, J. L., Ferry, D. K., and Tao, N. J., "Dielectric Screening Enhanced Performance in Graphene FET," *Nano Letters*, 9, 2571-2574, (2009).
- [12] Robinson, J. A., LaBella, M., Trumbull, K. A., Weng, X. J., Cavellero, R., Daniels, T., Hughes, Z., Hollander, M., Fanton, M., and Snyder, D., "Epitaxial Graphene Materials Integration: Effects of Dielectric Overlayers on Structural and Electronic Properties," *Acs Nano*, 4, 2667-2672, (2010).
- [13] Novoselov, K. S., Jiang, D., Schedin, F., Booth, T. J., Khotkevich, V. V., Morozov, S. V., and Geim, A. K., "Two-dimensional atomic crystals," *Proceedings of the National Academy of Sciences of the United States of America*, 102, 10451-10453, (2005).
- [14] Li, S. L., Miyazaki, H., Lee, M. V., Liu, C., Kanda, A., and Tsukagoshi, K., "Complementary-Like Graphene Logic Gates Controlled by Electrostatic Doping," *Small*, 7, 1552-1556, (2011).
- [15] Friedemann, M., Woszczyzna, M., Muller, A., Wundrack, S., Dziomba, T., Weimann, T., and Ahlers, F. J., "Versatile sputtering technology for Al<sub>2</sub>O<sub>3</sub> gate insulators on graphene," *Science and Technology of Advanced Materials*, 13, 025007, (2012).
- [16] Lee, J., Kim, J. H., and Im, S., "Pentacene thin-film transistors with Al<sub>2</sub>O<sub>3+x</sub> gate dielectric films deposited on indium-tin-oxide glass," *Applied Physics Letters*, 83, 2689-2691, (2003).
- [17] Lee, B. K., Park, S. Y., Kim, H. C., Cho, K., Vogel, E. M., Kim, M. J., Wallace, R. M., and Kim, J. Y., "Conformal Al<sub>2</sub>O<sub>3</sub> dielectric layer deposited by atomic layer deposition for graphene-based nanoelectronics," *Applied Physics Letters*, 92, (2008).
- [18] Graf, D., Molitor, F., Ensslin, K., Stampfer, C., Jungen, A., Hierold, C., and Wirtz, L., "Raman mapping of a single-layer to double-layer graphene transition," *European Physical Journal-Special Topics*, 148, 171-176, (2007).